Electronic Supplementary Material (ESI) for Journal of Materials Chemistry C.

Supporting Information

Regulating the miscibility of donor/acceptor to manipulate morphology and reduce non-radiative recombination energy loss enables efficient organic solar cells

Ziqi Han, Ke Wang, Yongqiang Chai, Rui Zhang*, Jianqi Zhang, Dan He*, Chunru Wang and Fuwen Zhao*

1. General characterization

^{1}H NMR and ^{13}C NMR spectra were measured on a Bruker Avance-400 spectrometer under room temperature. UV-vis absorption spectra were recorded on a UV-2600 UV-vis spectrophotometer (Shimadzu, Japan). Cyclic voltammetry was done by using a Shanghai Chenhua CHI660E voltammetric analyzer under argon in a solution of tetra-*n*-butylammonium hexafluorophosphate (0.1 M in acetonitrile). A glassy-carbon electrode was used as the working electrode, a platinum-wire was used as the counter electrode, and an Ag/AgCl electrode was used as the reference electrode. All potentials were corrected against Fc/Fc+ redox couple (Fc represents ferrocene.). The grazing incidence wide angle X-ray scattering (GIWAXS) measurements were conducted on an Xenocs-SAXS/WAXS system with an X-ray wavelength of 1.5418 Å and 0.2° as an incident angle. Pilatus 300 K was used as a 2D detector. All samples were prepared on the Si substrates using the same preparation conditions as for devices. AFM was performed on a Bruker Dimension icon by using tapping mode. All films were spin-coated onto ITO glass substrates. Contact angles of water and glycerol on donor and acceptor neat films were measured by the JY-82C contact angle analizer. The current density-voltage (*J-V*) curves were measured by using a Keithley 2450 source-measure unit in the nitrogen-filled glove box along the forward scan direction from -0.2 V to 1 V at room temperature. The scan speed and dwell times were fixed at 0.02 V per step and 0 ms, respectively. The photocurrent was measured under AM 1.5G illumination at 100 mW cm^{-2} by using a 3A solar simulator (LSS-55, JINZHU TECH, calibrated at 02/15/2022). Light intensity was calibrated with a standard photovoltaic cell equipped with a KG2 filter (certificated by the National PV Industry Measurement and Testing Center, 02/15/2022). The standard photovoltaic cell was calibrated in the range of 300-1200 nm with Urel = 1.3%. The EQE measurements of devices were carried out in the air with a solar cell spectral response measurement system (QE-R3018, Enli Technology Co., Ltd). The light intensity at each wavelength was calibrated by a standard single-crystal Si photovoltaic cell. The thicknesses of all films were measured by the Bruker Dektak-XT. Electroluminescence quantum efficiency (EQE_{EL}) measurements were performed by an integrated system (REPS, Enli Technology Co., Ltd.). EQE_{EL} measurements were carried out from 1 V to 4 V. Fourier-transform photocurrent spectroscopy external quantum efficiency (FTPS-EQE) was measured by an integrated system (PECT-600, Enli Technology Co., Ltd.), where the photocurrent was amplified and modulated by a lock-in instrument.

2. Synthesis

Unless stated otherwise, all solvents and chemical reagents were obtained commercially and used without further purification. The polymer donor, PM6 (Mw = 89 kDa, Mn = 37 kDa and PDI = 2.4), was purchased from Solarmer Materials Inc., 2-(5,6-dichloro-3-oxo-2,3-dihydro-1*H*-inden-1-ylidene)malononitrile was purchased from Derthon Co., and compound **1** was prepared according to the literature.[1]

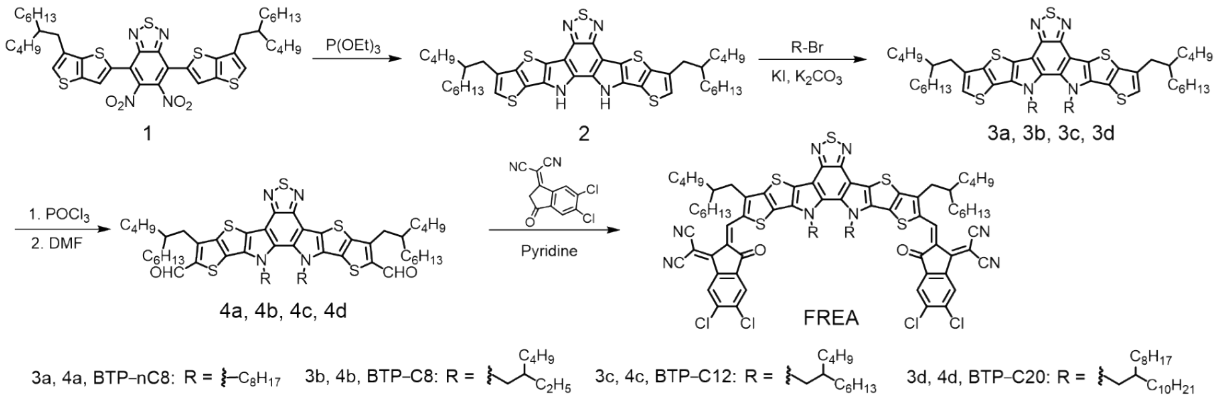

Fig. S1 The synthetic routes of BTP-nC8, BTP-C8, BTP-C12 and BTP-C20.

Compound 1. Compound **1** was prepared according to the literature.[1] ^{1}H NMR ($CDCl_3$, 400 MHz, δ/ppm): 7.71 (s, 2H), 7.15 (s, 2H), 2.71 (d, *J* = 7.0 Hz, 4H), 1.87 (s, 2H), 1.35-1.30 (m, 32H), 0.89-0.85 (s, 12H).

Compound 2. Under nitrogen atmosphere, triethyl phosphite (6.6 g) was added to the solution of compound **1** (1.8 g, 2.14 mmol) in *o*-dichlorobenzene (ODCB) (10 mL). The reaction mixture was heated to reflux under 180 °C and stirred overnight. After cooling down to room temperature, the solvent was removed under reduced pressure to obtain compound **2**, which was used for the next step directly.

Compound 3a. Bromooctane (1.5 g, 7.77 mmol), K_2CO_3 (1.06 g, 7.67 mmol) and KI (1.27 g, 7.65 mmol) were added to the three-necked flask (100 mL) with compound **2** in *N*, *N*-dimethylformamide (DMF) (25 mL) under Ar. The mixture was heated under 85 °C and stirred overnight. After cooling down to room temperature, the mixture was poured into water and extracted with dichloromethane for three times. The organic phase was combined and the solvent was removed under reduced pressure. Then, the residue was purified with silica gel column chromatography by using a mixture solvent of petroleum ether:dichloromethane (4:1) as the eluent to give the compound **3a** as an orange solid (693 mg, 32% yield on the basis of compound **1**). ^{1}H NMR ($CDCl_3$, 400 MHz, δ/ppm): 6.98 (s, 2H), 4.63-4.59 (m, 4H), 2.74 (d, *J* = 7.2 Hz, 4H), 1.99 (s, 2H), 1.88 (d, *J* = 7.5 Hz, 4H), 1.27-1.13 (m, 52H), 0.87-0.77 (m, 18H).

Compound 3b. 1-Bromo-2-ethylhexane (1.5 g, 7.77 mmol), K_2CO_3 (1.06 g, 7.67 mmol) and KI (1.27 g, 7.65 mmol) were added to the three-necked flask (100 mL) with compound **2** in *N*, *N*-dimethylformamide (DMF) (25 mL) under Ar. The mixture was heated under 85 °C and stirred overnight. After cooling down to room temperature, the mixture was poured into water and extracted with dichloromethane for three times. The organic phase was combined and the solvent was removed under reduced pressure. Then, the residue was purified with silica gel column chromatography by using a mixture solvent of petroleum ether:dichloromethane (4:1) as the eluent to give the compound **3b** as an orange solid (720 mg, 34% yield on the basis of compound **1**). ^{1}H NMR ($CDCl_3$, 400 MHz, δ/ppm): 6.99 (s, 2H), 4.60 (d, *J* = 7.7 Hz, 4H), 2.75 (d, *J* = 7.2 Hz, 4H), 2.13-1.88 (m, 4H), 1.36-1.24 (m, 36H), 0.90-0.85 (m, 24H), 0.66-0.62 (m, 6H), 0.59 (t, *J* = 7.2 Hz, 6H).

Compound 3c. 1-Bromo-2-butyloctane (1.34 g, 5.38 mmol), K_2CO_3 (740.8 mg, 5.36 mmol) and KI (889.8 mg, 5.36 mmol) were added to the three-necked flask (100 mL) with compound **2** in *N*, *N*-dimethylformamide (DMF) (25 mL) under Ar. The mixture was heated under 85 °C and stirred overnight. After cooling down to room temperature, the mixture was poured into water and extracted with dichloromethane for three times. The organic phase was combined and the solvent was removed under reduced pressure. Then, the residue was purified with silica gel column chromatography by using a mixture solvent of petroleum ether:dichloromethane (4:1) as the eluent to give the compound **3c** as an orange cream (845 mg, 35% yield on the basis of compound **1**). ^{1}H NMR ($CDCl_3$, 400 MHz, δ/ppm): 6.99 (s, 2H), 4.59 (d, *J* = 7.8 Hz, 4H), 2.75 (d, *J* = 7.2 Hz, 4H), 2.06 (s, 2H), 1.99 (s, 2H), 1.34-1.25 (m, 38H), 0.99-0.82 (m, 38H), 0.65-0.56 (m, 12H).

Compound 3d. 1-Bromo-2-octyldodecane (1.93 g, 5.34 mmol), K_2CO_3 (740.8 mg, 5.36 mmol) and KI (889.8 mg, 5.36 mmol) were added to the three-necked flask (100 mL) with compound **2** in *N*, *N*-dimethylformamide (DMF) (25 mL) under Ar. The mixture was heated under 85 °C and stirred overnight. After cooling down to room temperature, the mixture was poured into water and extracted with dichloromethane for three times. The organic phase was combined and the solvent was removed under reduced pressure. Then, the residue was purified with silica gel column chromatography by using a mixture solvent of petroleum ether:dichloromethane (4:1) as the eluent to give the compound **3d** as an orange cream (890 mg, 31% yield on the basis of compound **1**). ^{1}H NMR ($CDCl_3$, 400 MHz, δ/ppm): 6.98 (s, 2H), 4.58 (d, *J* = 7.7 Hz, 4H),

2.74 (d, J = 7.1 Hz, 4H), 2.10-2.03 (m, 2H), 1.99 (s, 2H), 1.37-1.14 (m, 54H), 1.09-0.93 (m, 27H), 0.91-0.85 (m, 30H), 0.82 (t, J = 7.2 Hz, 9H).

Compound 4a. Under Ar, $POCl_3$ (0.2 mL) was added dropwise to anhydrous DMF (0.5 mL) under 0 °C and stirred at room temperature for 2 hours. Then, compound **3a** (210 mg, 0.21 mmol), dissolved in 1,2-dichloroethane (6 mL), was added into the mixture and stirred at 85 ºC overnight. After cooling down to room temperature, the mixture was poured into water and extracted with dichloromethane for three times. The obtained crude product was further purified by silica gel column chromatography with a mixture solvent of petroleum ether: dichloromethane (1:1) as the eluent to give the compound **4a** as an orange solid (180 mg, 81% yield). ^{1}H NMR ($CDCl_3$, 400 MHz, δ/ppm): 10.11 (s, 2H), 4.66 (t, J = 7.7 Hz, 4H), 3.09 (d, J = 7.4 Hz, 4H), 2.06 (s, 2H), 1.90 (s, 4H), 1.41-1.11 (m, 52H), 0.90-0.77 (m, 18H). ^{13}C NMR ($CDCl_3$, 100 MHz, δ/ppm): 182.02, 147.50, 146.47, 143.30, 137.71, 136.74, 132.67, 129.47, 127.18, 112.30, 55.06, 40.04, 39.14, 33.78, 33.46, 33.16, 31.79, 29.59, 29.40, 28.77, 27.43, 27.36, 26.56, 22.97, 22.66, 22.62, 14.09, 13.65, 10.15, 10.06.

Compound 4b. Under Ar, $POCl_3$ (0.2 mL) was added dropwise to a solution of anhydrous DMF (0.5 mL) under 0 °C and stirred at room temperature for 2 hours. Then, compound **3b** (206 mg, 0.206 mmol), dissolved in 1,2-dichloroethane (6 mL), was added to the mixture and stirred at 85 ºC overnight. After cooling down to room temperature, the mixture was poured into water and extracted with dichloromethane for three times. The obtained crude product was further purified by silica gel column chromatography with a mixture solvent of petroleum ether: dichloromethane (1:1) as the eluent to give the compound **4b** as an orange solid (190 mg, 87% yield) ^{1}H NMR ($CDCl_3$, 400 MHz, δ/ppm): 10.12 (s, 2H), 4.64 (d, J = 7.8 Hz, 4H), 3.11 (d, J = 7.5 Hz, 4H), 2.10-1.98 (m, 4H), 1.45-1.19 (m, 34H), 1.03-0.83 (m, 26H), 0.67 (q, J = 7.5 Hz, 6H), 0.59 (q, J = 7.1 Hz, 6H). ^{13}C NMR ($CDCl_3$, 100 MHz, δ/ppm): 181.80, 147.05, 146.19, 143.09, 137.54, 136.45, 131.44, 128.89, 126.90, 112.15, 50.88, 39.10, 33.68, 33.38, 32.97, 31.80, 31.61, 31.27, 29.61, 29.09, 28.70, 26.51, 22.98, 22.63, 22.53, 14.08, 14.02.

Compound 4c. Under Ar, $POCl_3$ (0.2 mL) was added dropwise to a solution of anhydrous DMF (0.5 mL) under 0 °C and stirred at room temperature for 2 hours. Then, compound **3c** (220 mg, 0.198 mmol), dissolved in 1,2-dichloroethane (6 mL), was added to the mixture and stirred at 85 ºC overnight. After cooling down to room temperature, the mixture was poured into water and extracted with dichloromethane for three times. The obtained crude product was further purified by silica gel column chromatography with a mixture solvent of petroleum ether: dichloromethane (1:1) as an eluent to give the compound **4c** as an orange cream (200 mg, 87% yield). ^{1}H NMR ($CDCl_3$, 400 MHz, δ/ppm): 10.11 (s, 2H), 4.61 (d, J = 7.9 Hz, 4H), 3.10 (d, J = 7.4 Hz, 4H), 2.09-2.01 (m, 4H), 1.42-1.24 (m, 38H), 0.96-0.80 (m, 38H), 0.66-0.58 (m, 12H). ^{13}C NMR ($CDCl_3$, 100 MHz, δ/ppm): 182.01, 147.44, 146.44, 143.31, 137.71, 136.70, 132.87, 129.49, 127.39, 112.29, 55.17, 39.13, 38.79, 33.74, 33.42, 33.13, 31.80, 31.44, 31.39, 30.13, 29.59, 29.25, 28.74, 27.73, 27.59, 26.54, 25.19, 25.04, 22.97, 22.64, 22.39, 14.08, 13.92, 13.67.

Compound 4d. Under Ar, $POCl_3$ (0.2 mL) was added dropwise to anhydrous DMF (0.5 mL) under 0 °C and stirred at room temperature for 2 hours. Then, compound **3d** (200 mg, 0.15 mmol), dissolved in 1,2-dichloroethane (6 mL), was added into the mixture and stirred at 85 ºC overnight. After cooling down to room temperature, the mixture was poured into water and extracted with dichloromethane for three times. The obtained crude product was further purified by silica gel column chromatography with a mixture solvent of petroleum ether: dichloromethane (1:1) as the eluent to give the compound **4d** as an orange cream (150 mg, 72% yield). ^{1}H NMR ($CDCl_3$, 400 MHz, δ/ppm): 10.12 (s, 2H), 4.62 (d, J = 7.8 Hz, 4H), 3.11 (d, J = 7.4 Hz, 4H), 2.06 (s, 4H), 1.43-1.23 (m, 42H), 1.20-0.93 (m, 54H), 0.89-0.80 (m, 24H). ^{13}C NMR ($CDCl_3$, 100 MHz, δ/ppm): 181.94, 147.43, 146.37, 143.32, 137.72, 136.73, 132.84, 129.48, 127.35, 112.33, 55.21, 39.11, 38.80, 33.76, 33.44, 33.11, 31.89, 31.81, 31.73, 30.26,

29.62, 29.51, 29.46, 29.30, 29.28, 29.24, 29.11, 28.74, 26.53, 25.38, 22.98, 22.68, 22.63, 22.58, 14.14, 14.10, 14.08.

BTP-nC8. Compound **4a** (100 mg, 0.0947 mmol) and 2-(5,6-dichloro-3-oxo-2,3-dihydro-1*H*-inden-1-ylidene) malononitrile (99.7 mg, 0.379 mmol) were added into chloroform (10 mL) under Ar. After stirring at room temperature for 10 min, pyridine (1 mL) was added. The reaction mixture was allowed to stir at 65 ºC for 1 hour. After cooling down to room temperature, methanol was added and the precipitate was collected by filtration to get the crude product, which was further purified by silica gel column chromatography with chloroform as the eluent to afford BTP-nC8 as a dark solid (100 mg, 68% yield). ^{1}H NMR ($CDCl_3$, 400 MHz, δ/ppm): 8.69 (s, 2H), 8.67 (s, 2H), 7.81 (s, 2H), 4.71-4.62 (m, 4H), 2.88 (d, *J* = 7.7 Hz, 4H), 2.14 (s, 4H), 1.92 (s, 2H), 1.55 (s, 4H), 1.41-1.16 (m, 48H), 0.90-0.81 (m, 18H). ^{13}C NMR ($CDCl_3$, 100 MHz, δ/ppm): 185.78, 157.36, 153.57, 146.86, 145.34, 139.25, 138.77, 138.29, 137.06, 135.60, 134.85, 134.30, 133.97, 132.04, 130.54, 126.57, 124.31, 119.59, 114.87, 114.40, 113.26, 69.15, 51.30, 39.72, 34.69, 33.48, 33.22, 31.91, 31.86, 31.80, 29.68, 29.60, 29.49, 28.89, 27.20, 26.65, 22.98, 22.71, 22.63, 14.16, 14.08, 14.05. MALDI-TOF MS (m/z): 1544.865 $[M]^+$, calcd. for $C_{84}H_{90}Cl_4N_8O_2S_5$ (1544.451).

BTP-C8. Compound **4b** (80 mg, 0.0758 mmol) and 2-(5,6-dichloro-3-oxo-2,3-dihydro-1*H*-inden-1-ylidene) malononitrile (79.8 mg, 0.303 mmol) were added into chloroform (10 mL) under Ar. After stirring at room temperature for 10 min, pyridine (1 mL) was added. The reaction mixture was allowed to stir at 65 ºC for 1 hour. After cooling down to room temperature, methanol was added and the precipitate was collected by filtration to get the crude product, which was further purified by silica gel column chromatography with chloroform as the eluent to afford BTP-C8 as a dark solid (81 mg, 69% yield). ^{1}H NMR ($CDCl_3$, 400 MHz, δ/ppm): 9.17 (s, 2H), 8.80 (s, 2H), 7.98 (s, 2H), 4.78 (d, *J* = 7.9 Hz, 4H), 3.18 (d, *J* = 7.6 Hz, 4H), 2.09 (s, 4H), 1.47-1.19 (m, 36H), 1.05-0.83 (m, 24H), 0.77 (dd, *J* = 7.2, 3.0 Hz, 6H), 0.64 (dd, *J* = 7.3, 3.6 Hz, 6H). ^{13}C NMR ($CDCl_3$, 100 MHz, δ/ppm): 186.12, 158.98, 153.76, 147.57, 145.48, 139.55, 139.16, 138.74, 137.70, 136.23, 136.09, 135.99, 134.38, 133.98, 126.89, 125.01, 124.50, 120.10, 114.56, 113.81, 113.65, 68.83, 57.79, 41.27, 40.01, 34.57, 33.63, 33.37, 31.47, 29.70, 29.62, 28.86, 27.90, 27.66, 23.31, 22.99, 22.77, 22.63, 21.35, 14.07, 13.22, 10.27. MALDI-TOF MS (m/z): 1544.972 $[M]^+$, calcd. for $C_{84}H_{90}Cl_4N_8O_2S_5$ (1544.451).

BTP-C12. Compound **4c** (120 mg, 0.103 mmol) and 2-(5,6-dichloro-3-oxo-2,3-dihydro-1*H*-inden-1-ylidene) malononitrile (90.7 mg, 0.34 mmol) were added into chloroform (10 mL) under Ar. After stirring at room temperature for 10 min, pyridine (1 mL) was added. The reaction mixture was allowed to stir at 65 ºC for 1 hour. After cooling down to room temperature, methanol was added and the precipitate was collected by filtration to get the crude product, which was further purified by silica gel column chromatography with chloroform as the eluent to afford BTP-C12 as a dark solid (120 mg, 70% yield). ^{1}H NMR ($CDCl_3$, 400 MHz, δ/ppm): 9.17 (s, 2H), 8.80 (s, 2H), 7.96 (s, 2H), 4.76 (d, *J* = 7.5 Hz, 4H), 3.18 (d, *J* = 7.5 Hz, 4H), 2.10 (dd, *J* = 12.8, 6.0 Hz, 4H), 1.37-1.21 (m, 38H), 0.97-0.82 (m, 38H), 0.71-0.60 (m, 12H). ^{13}C NMR ($CDCl_3$, 100 MHz, δ/ppm): 186.06, 158.99, 153.72, 147.54, 145.48, 139.53, 139.16, 138.74, 137.60, 136.22, 136.11, 136.05, 134.45, 134.28, 131.26, 126.90, 124.94, 120.09, 115.20, 114.58, 113.60, 68.81, 55.81, 40.11, 39.24, 34.79, 33.61, 33.33, 31.84, 31.56, 30.58, 30.42, 29.70, 29.63, 29.40, 28.84, 27.83, 26.58, 25.50, 22.99, 22.76, 22.63, 22.45, 14.07, 14.04, 13.71. MALDI-TOF MS (m/z): 1657.061 $[M]^+$, calcd. for $C_{92}H_{106}Cl_4N_8O_2S_5$ (1656.577).

BTP-C20. Compound **4d** (100 mg, 0.0718 mmol) and 2-(5,6-dichloro-3-oxo-2,3-dihydro-1*H*-inden-1-ylidene) malononitrile (90.0 mg, 0.342 mmol) were added into chloroform (10 mL) under Ar. After stirring at room temperature for 10 min, pyridine (1 mL) was added. The reaction mixture was allowed to stir at 65 ºC for 1 hour. After cooling down to room temperature, methanol was added and the precipitate was collected by filtration to get the crude

product, which was further purified by silica gel column chromatography with chloroform as the eluent to afford BTP-C20 as a dark solid (99 mg, 73% yield). ^{1}H NMR ($CDCl_3$, 400 MHz, δ/ppm): 9.18 (s, 2H), 8.81 (s, 2H), 7.87 (s, 2H), 4.76 (d, J = 7.8 Hz, 4H), 3.20 (d, J = 7.6 Hz, 4H), 2.09 (s, 4H), 1.50-0.93 (m, 96H), 0.87-0.77 (m, 24H). ^{13}C NMR ($CDCl_3$, 100 MHz, δ/ppm): 185.90, 158.66, 153.64, 147.54, 145.45, 139.39, 139.05, 138.66, 137.60, 136.21, 135.99, 135.93, 134.42, 134.32, 131.27, 126.76, 124.81, 119.86, 115.24, 114.59, 113.61, 68.64, 55.95, 39.99, 39.31, 34.61, 33.59, 33.31, 31.90, 31.85, 31.81, 30.76, 30.73, 29.79, 29.76, 29.63, 29.61, 29.55, 29.42, 29.36, 29.33, 29.19, 28.80, 26.55, 25.76, 22.95, 22.66, 22.61, 14.07, 14.06, 14.00. MALDI-TOF MS (m/z): 1882.109 $[M]^+$, calcd. for $C_{108}H_{138}Cl_4N_8O_2S_5$ (1881.830).

3. NMR spectra

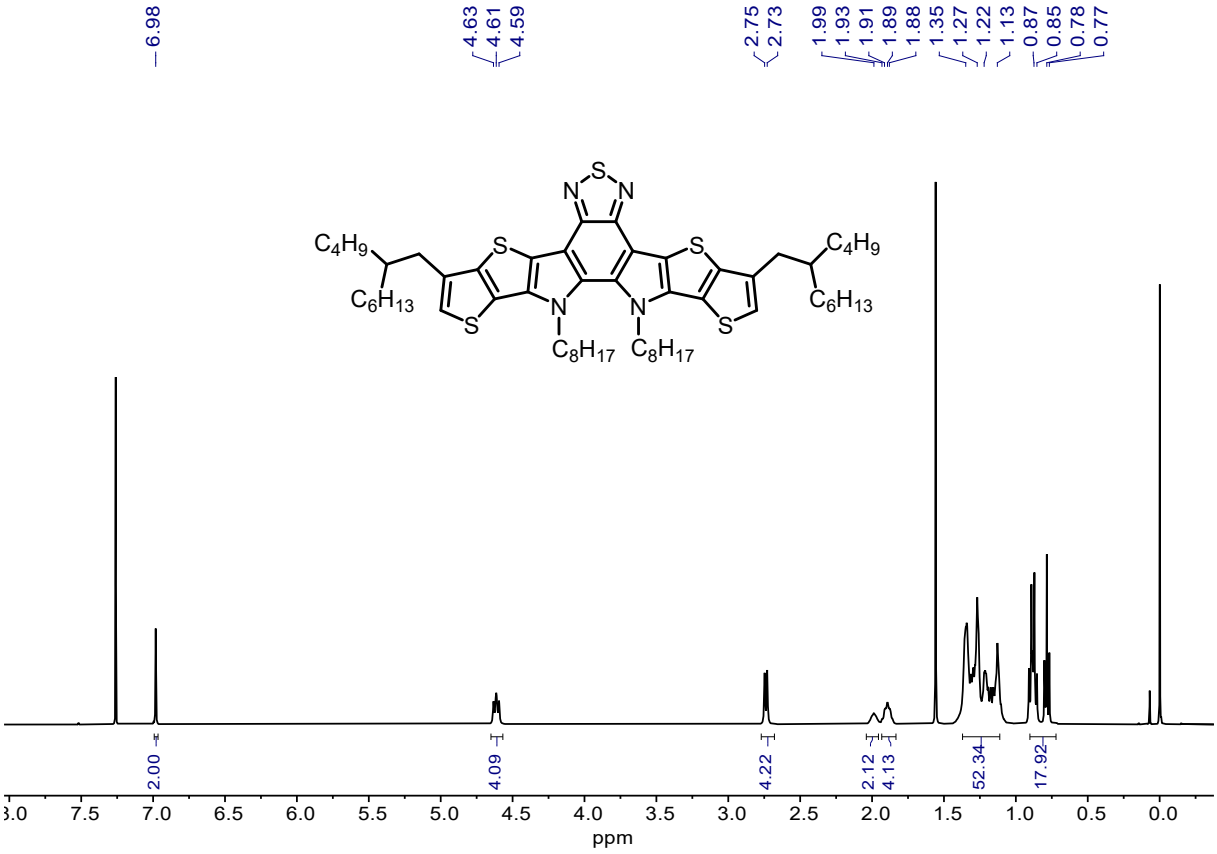

Fig. S2 ^{1}H NMR spectrum of compound **3a** in $CDCl_3$.

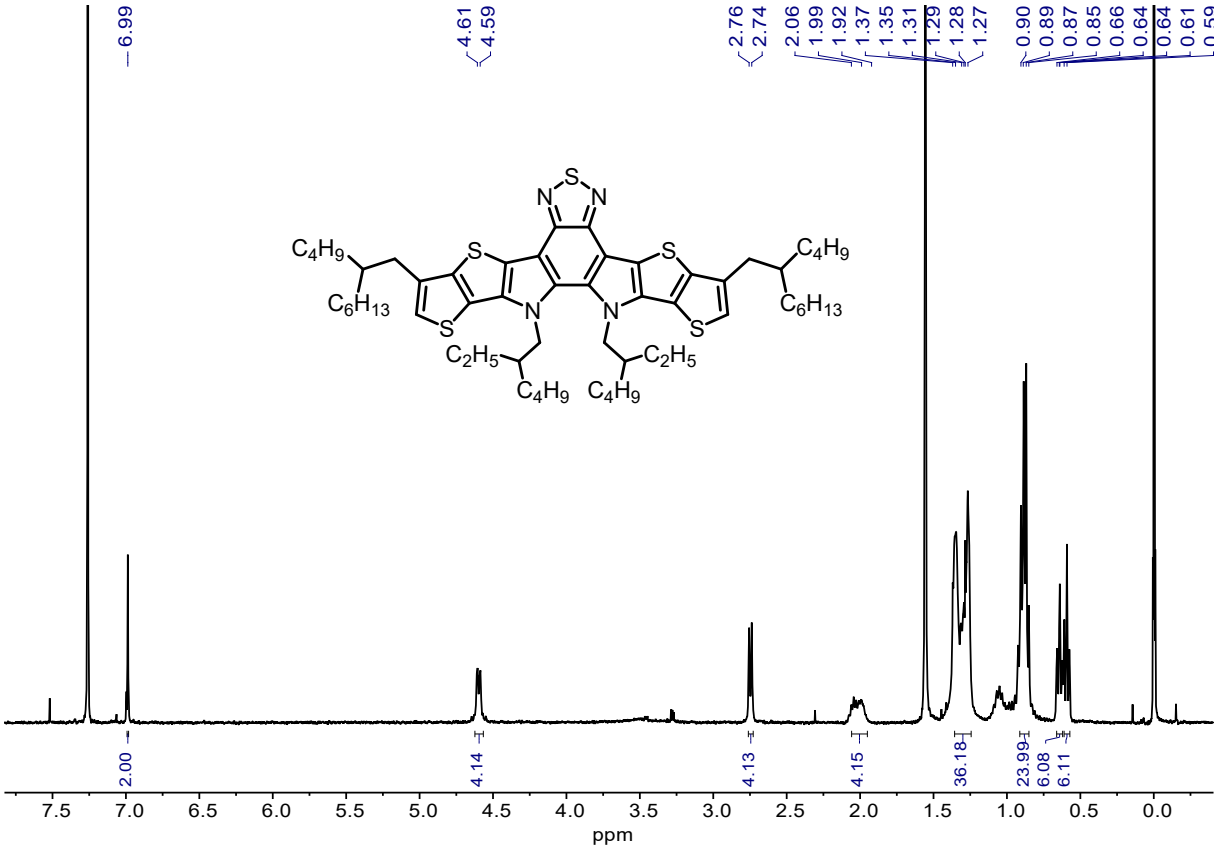

Fig. S3 ^{1}H NMR spectrum of compound **3b** in $CDCl_3$.

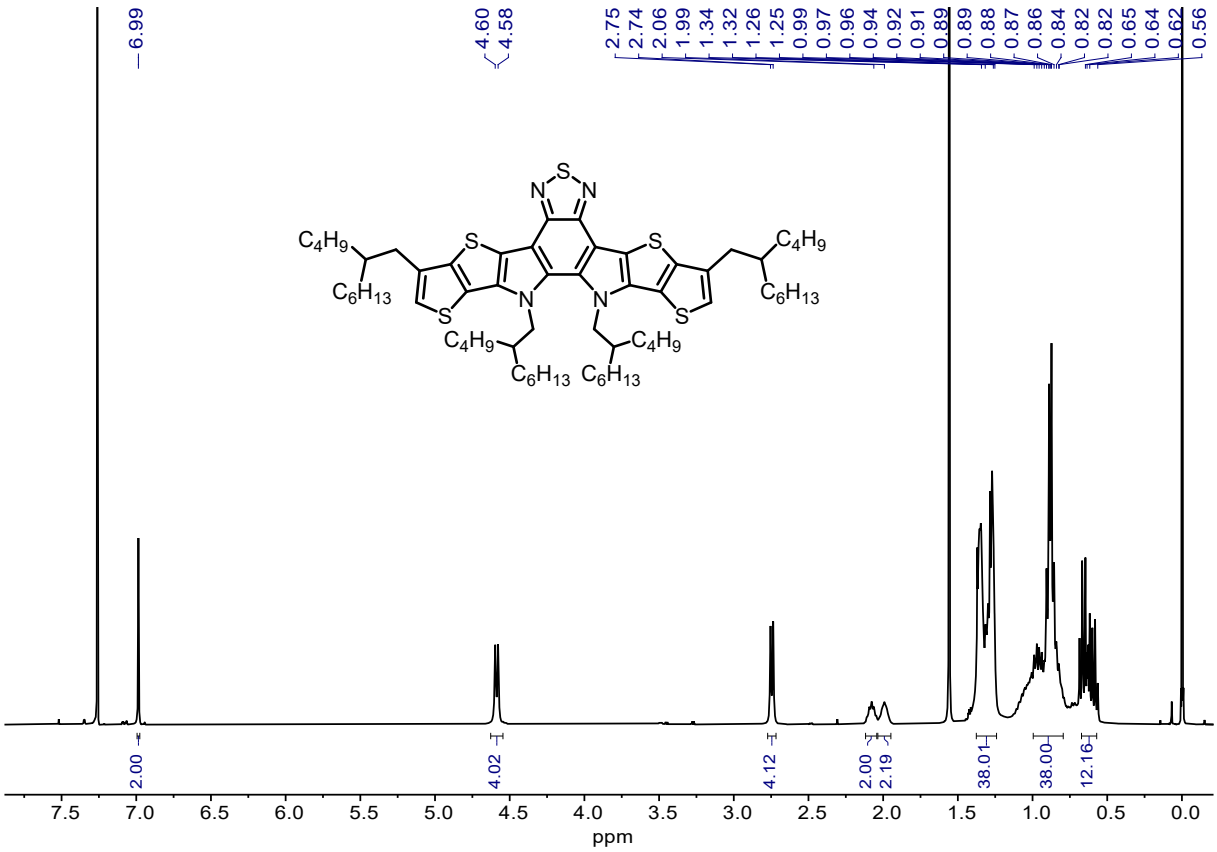

Fig. S4 ^{1}H NMR spectrum of compound **3c** in $CDCl_3$.

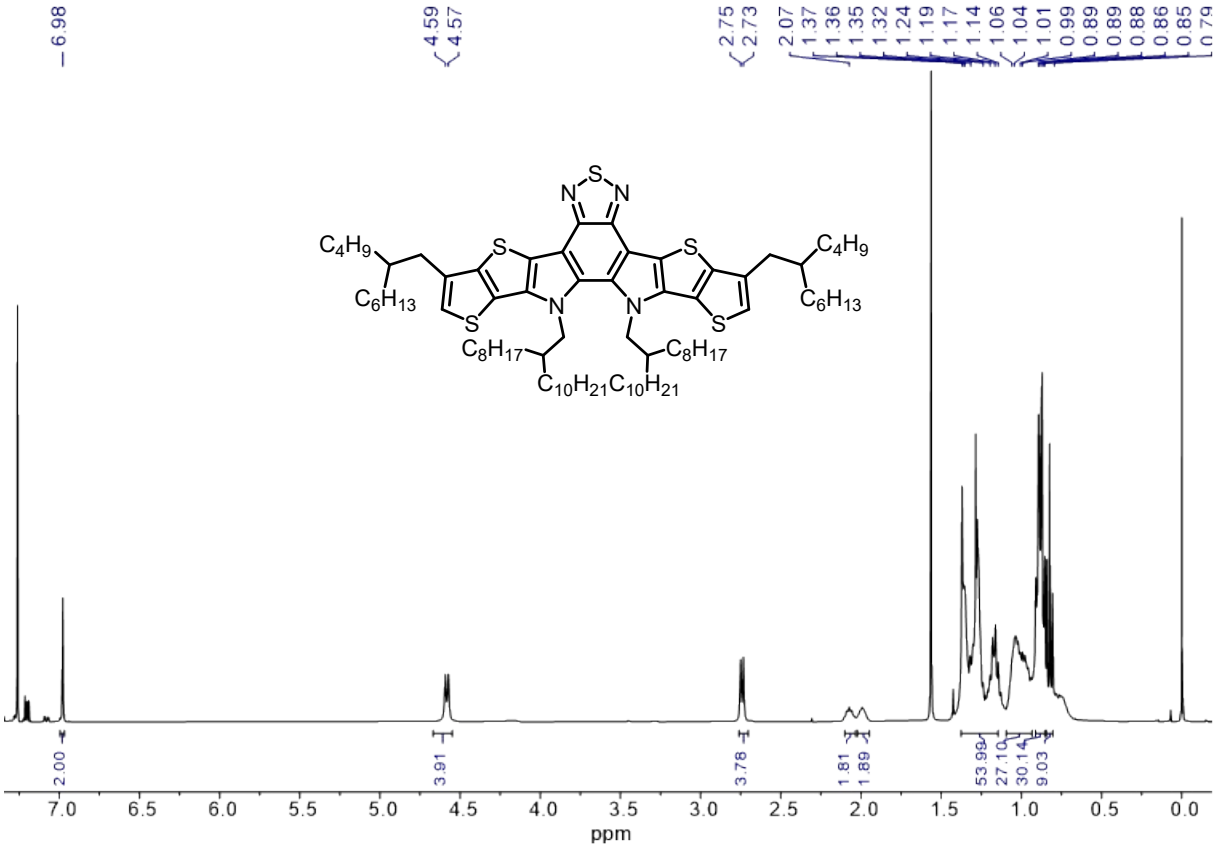

Fig. S5 ^{1}H NMR spectrum of compound **3d** in $CDCl_3$.

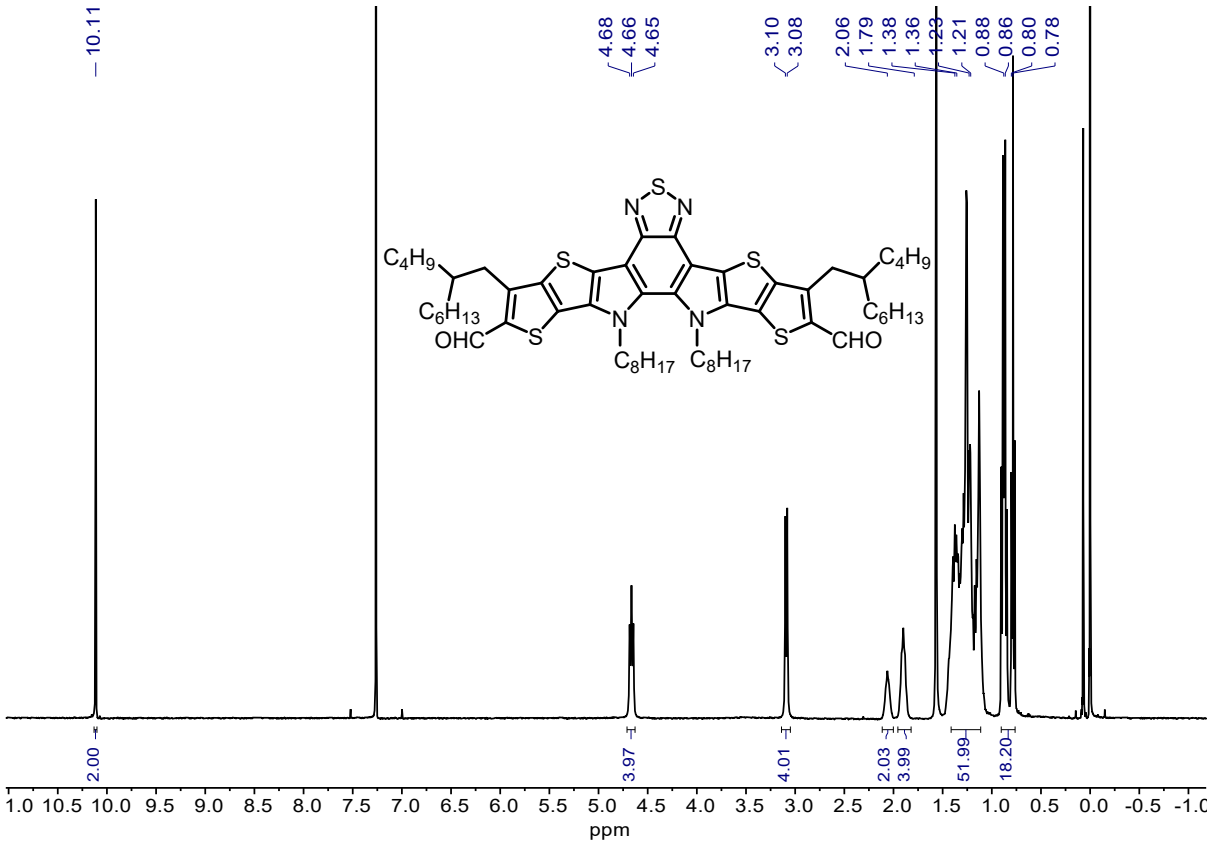

Fig. S6 ^{1}H NMR spectrum of compound **4a** in $CDCl_3$.

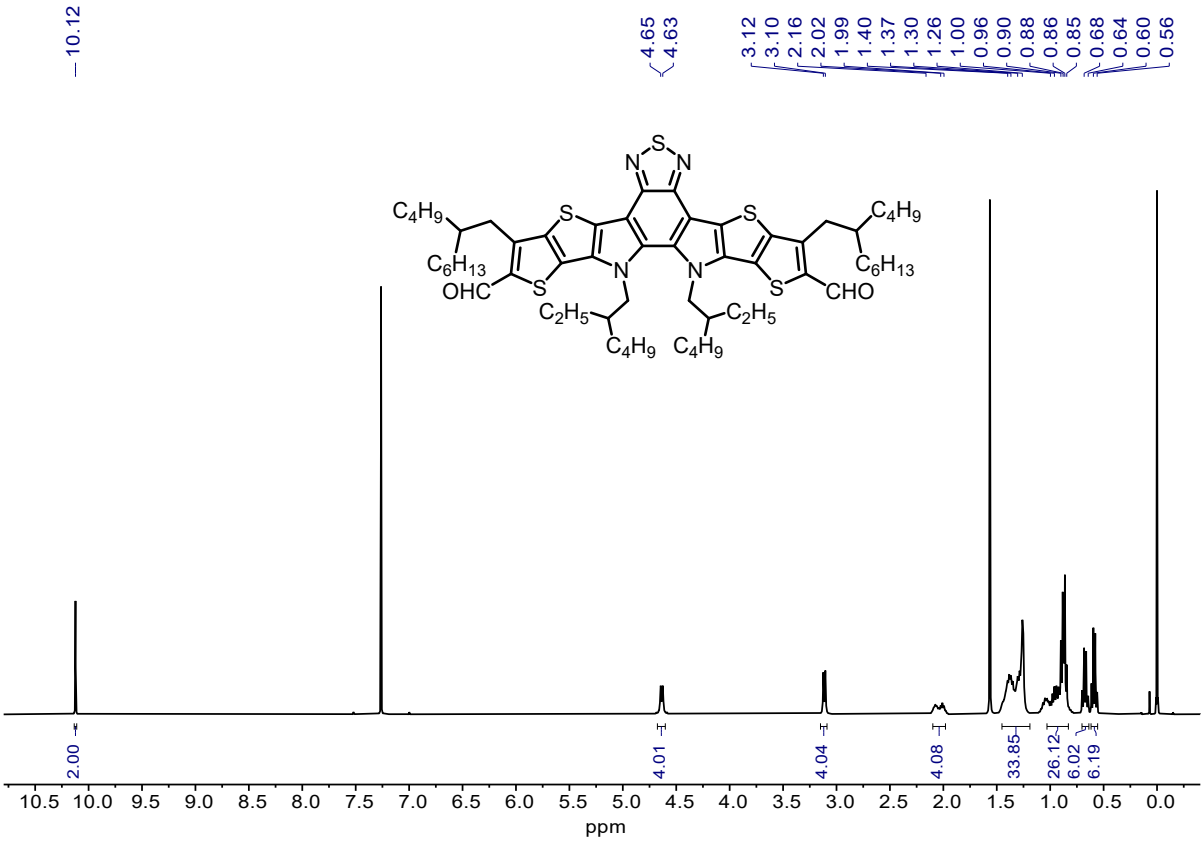

Fig. S7 ^{1}H NMR spectrum of compound **4b** in $CDCl_3$.

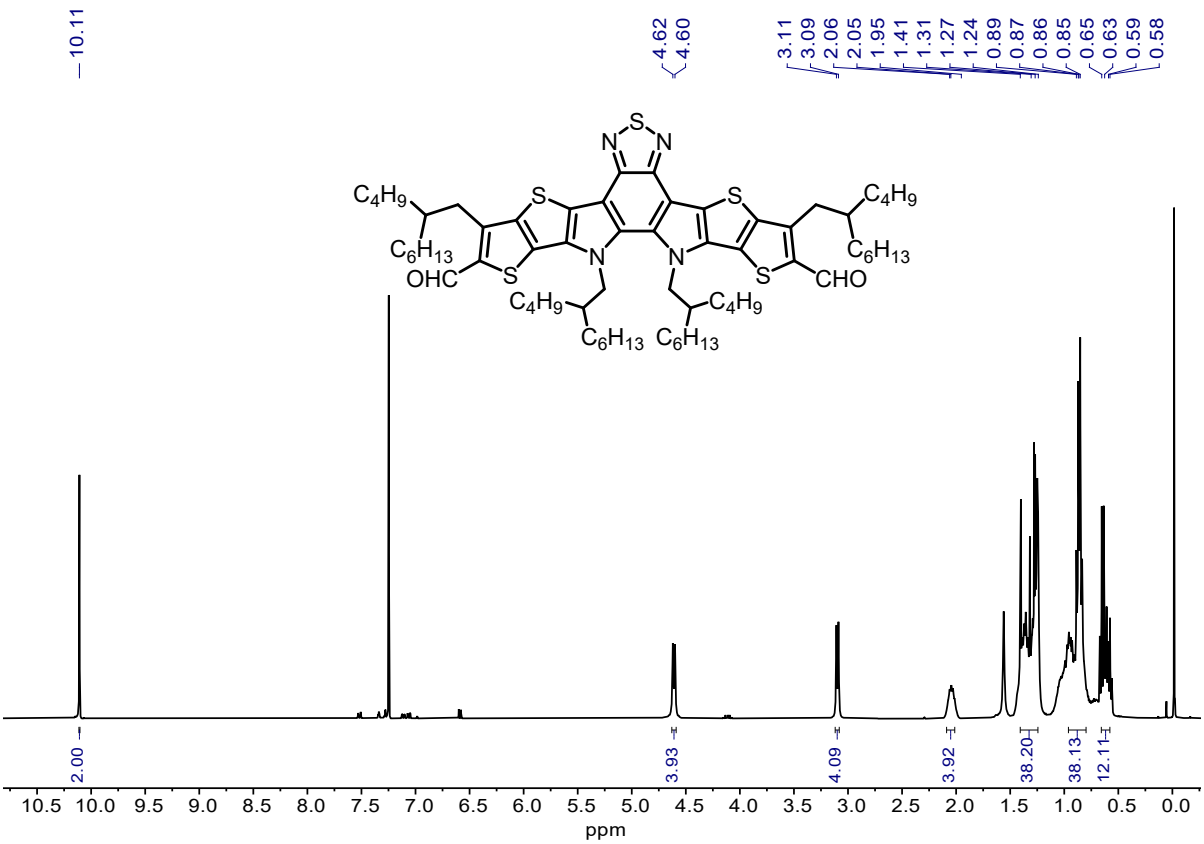

Fig. S8 ^{1}H NMR spectrum of compound **4c** in $CDCl_3$.

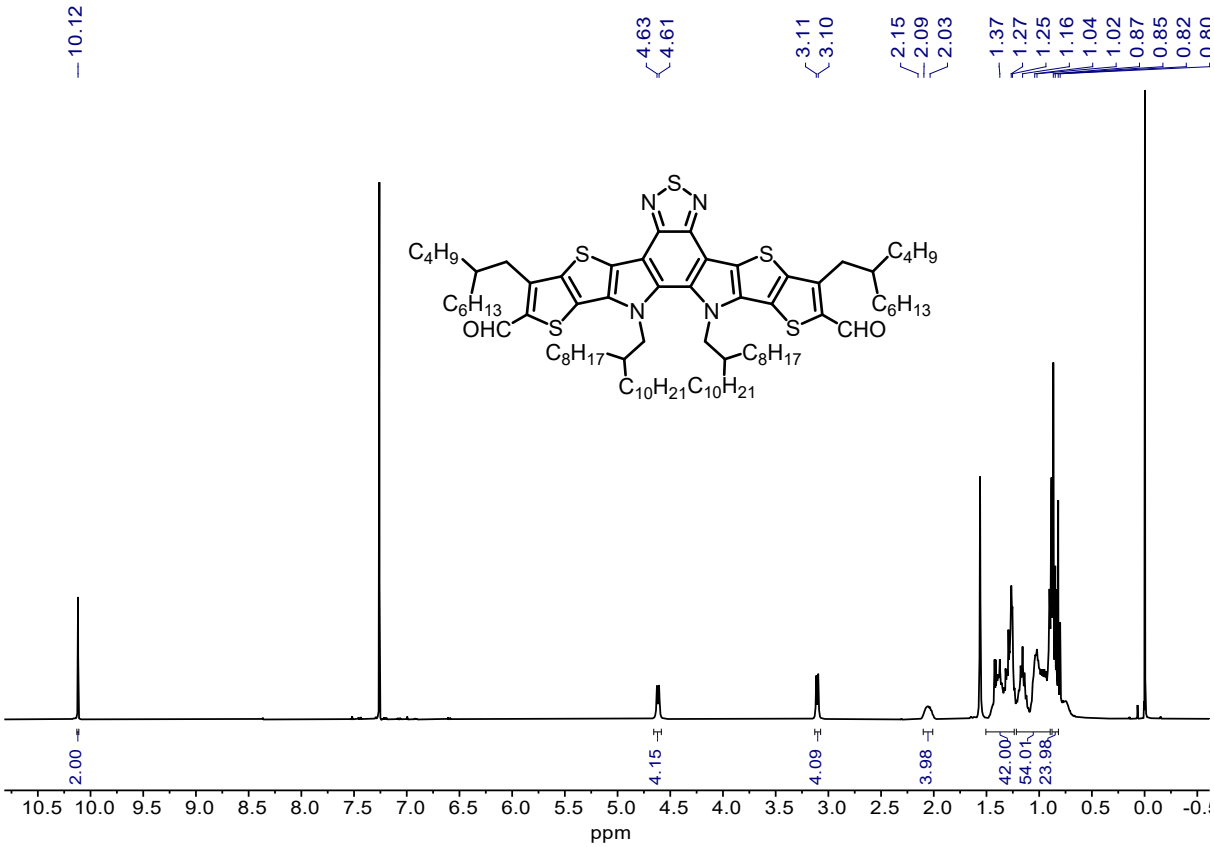

Fig. S9 ^{1}H NMR spectrum of compound **4d** in $CDCl_3$.

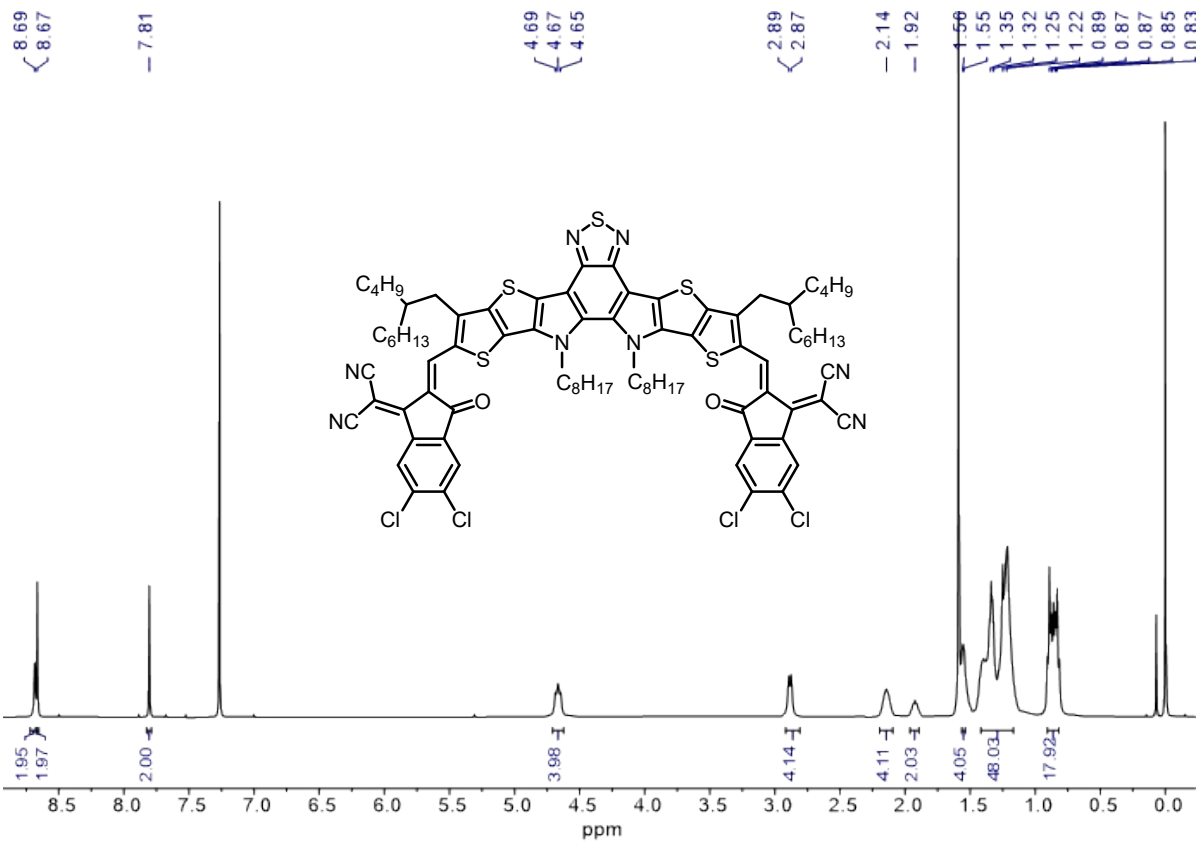

Fig. S10 ^{1}H NMR spectrum of BTP-nC8 in $CDCl_3$.

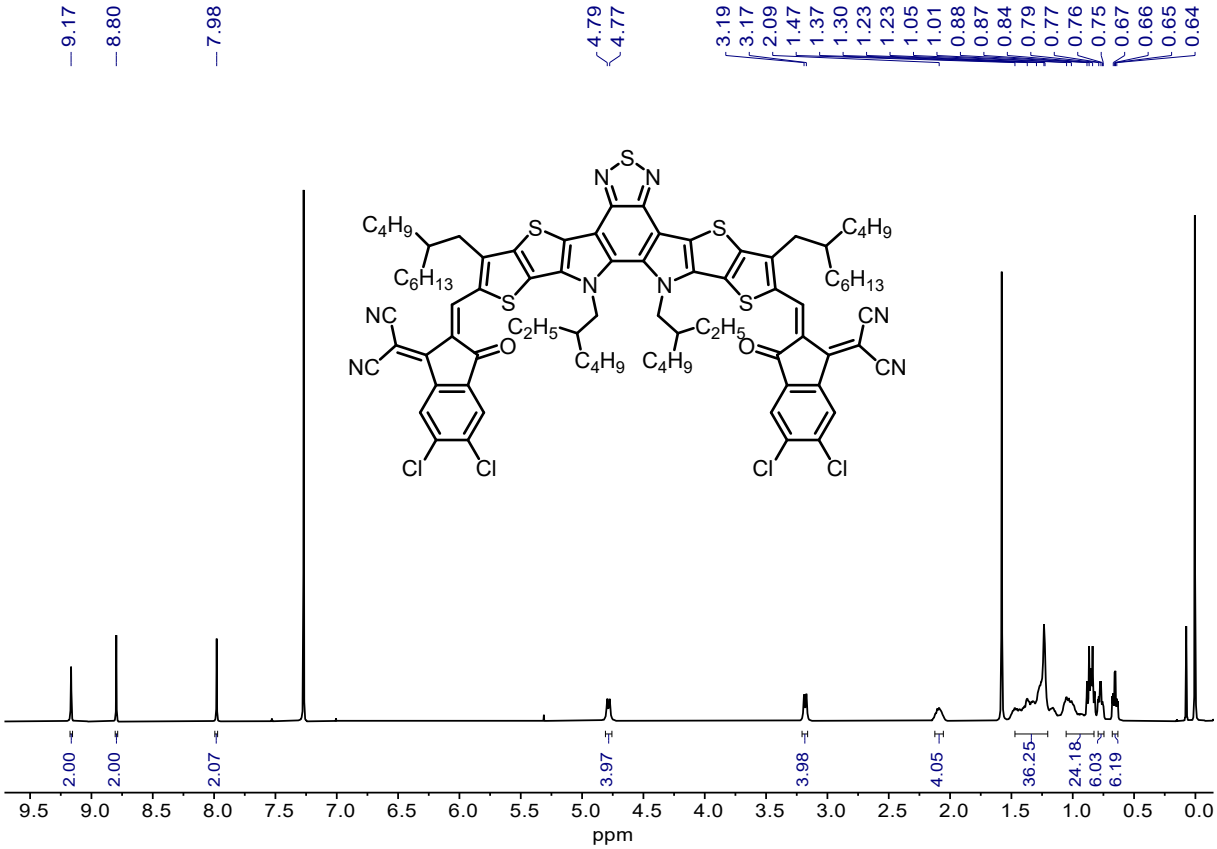

Fig. S11 ^{1}H NMR spectrum of BTP-C8 in $CDCl_3$.

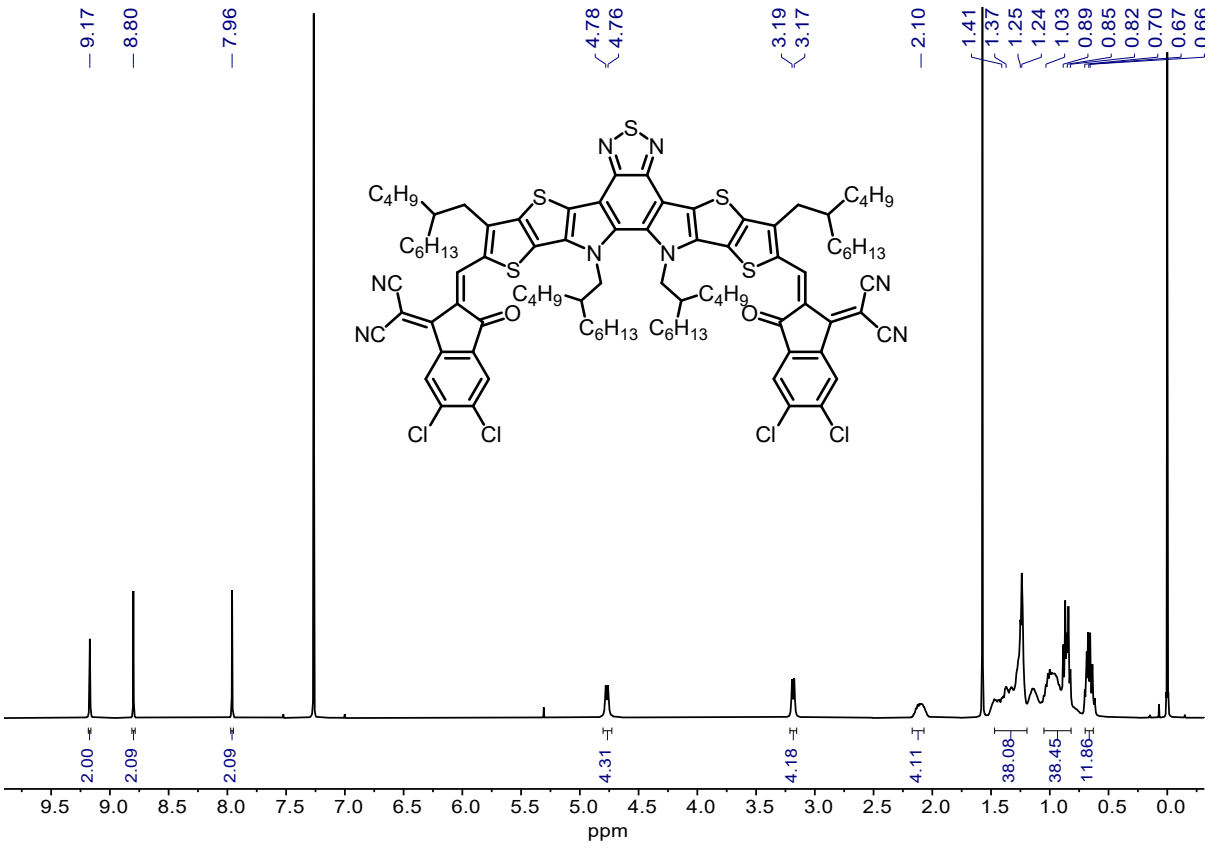

Fig. S12 ^{1}H NMR spectrum of BTP-C12 in $CDCl_3$.

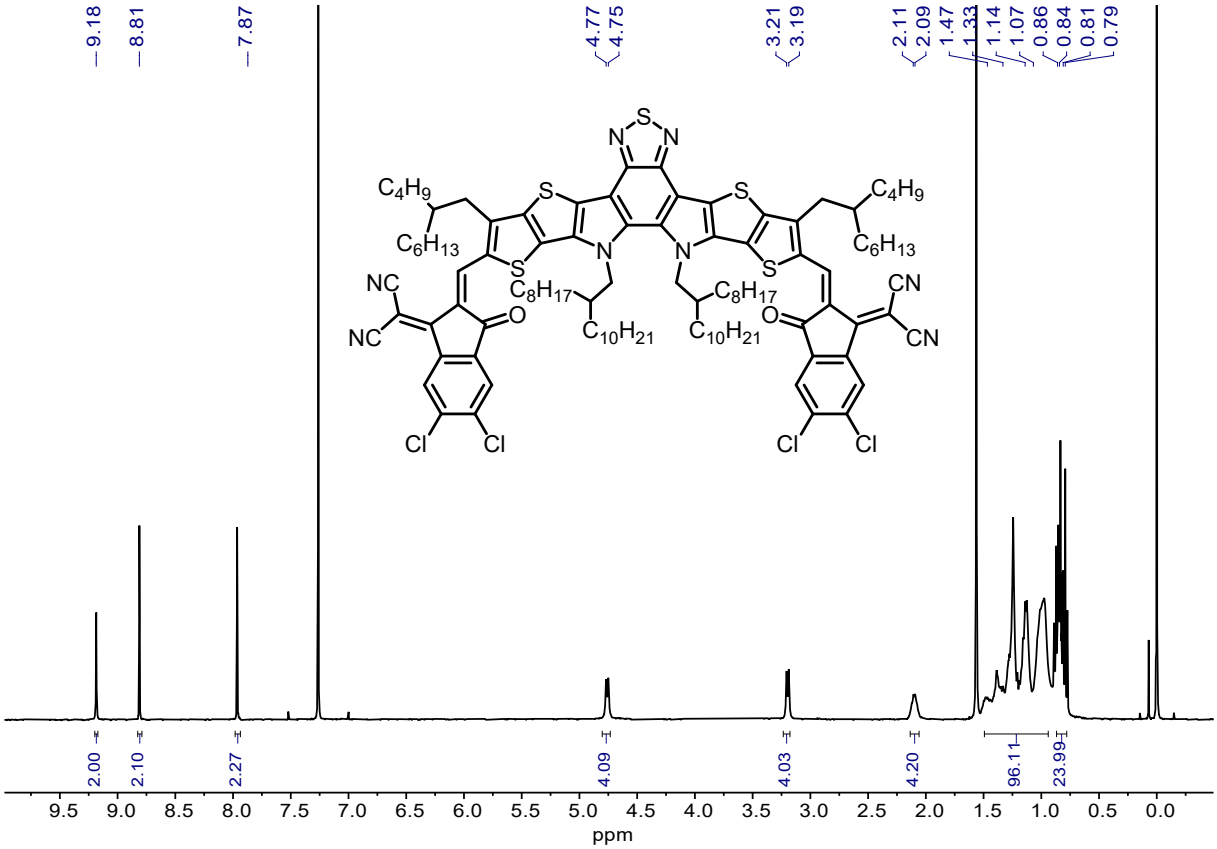

Fig. S13 ^{1}H NMR spectrum of BTP-C20 in $CDCl_3$.

4. Mass spectra

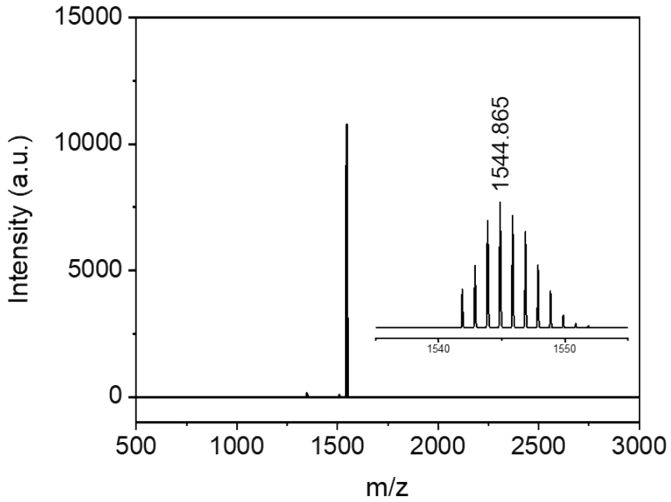

Fig. S14 Mass spectrum of BTP-nC8.

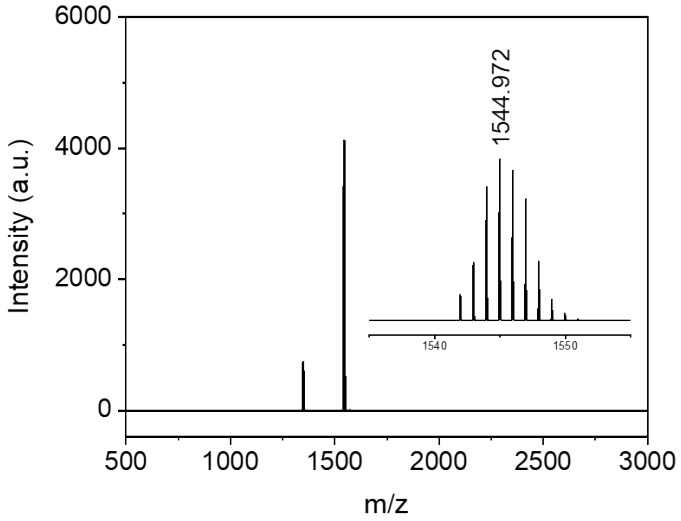

Fig. S15 Mass spectrum of BTP-C8.

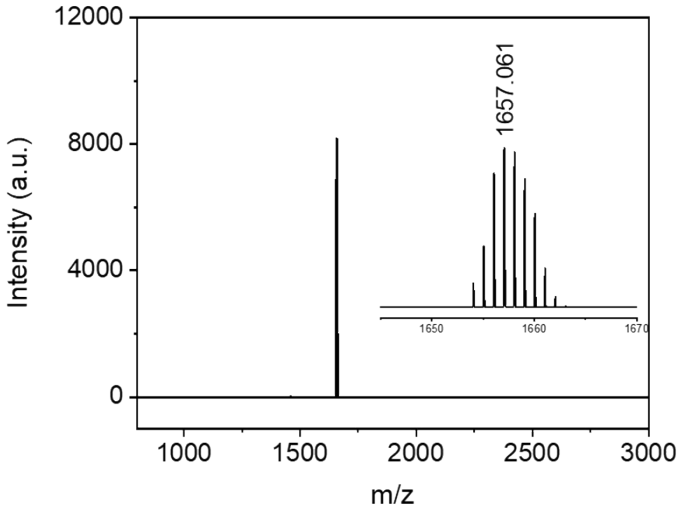

Fig. S16 Mass spectrum of BTP-C12.

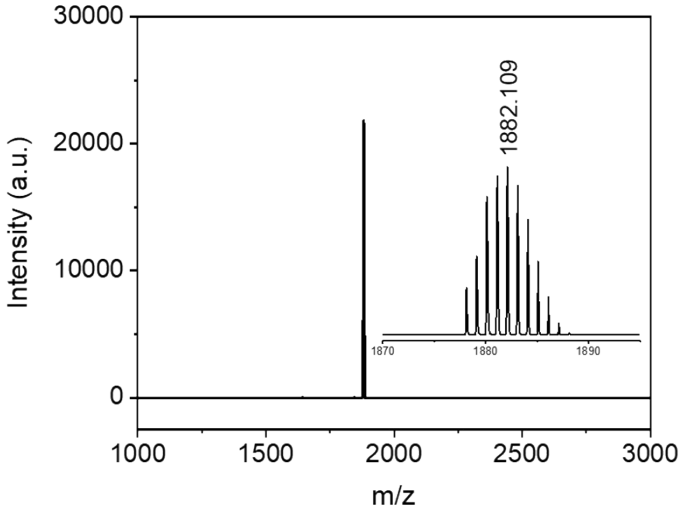

Fig. S17 Mass spectrum of BTP-C20.

5. Cyclic voltammetry

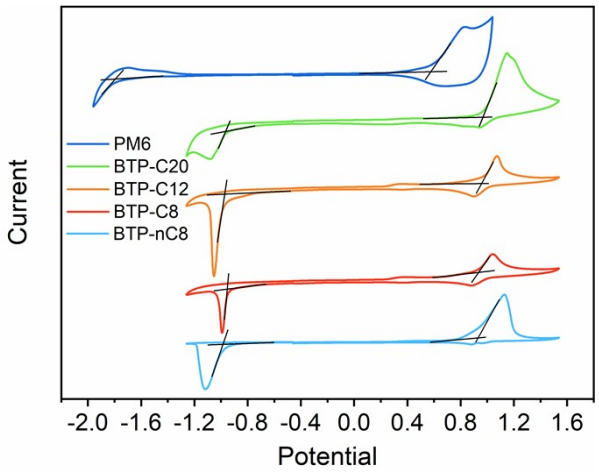

Fig. S18 Cyclic voltammograms of PM6, BTP-nC8, BTP-C8, BTP-C12 and BTP-C20.

6. Absorption

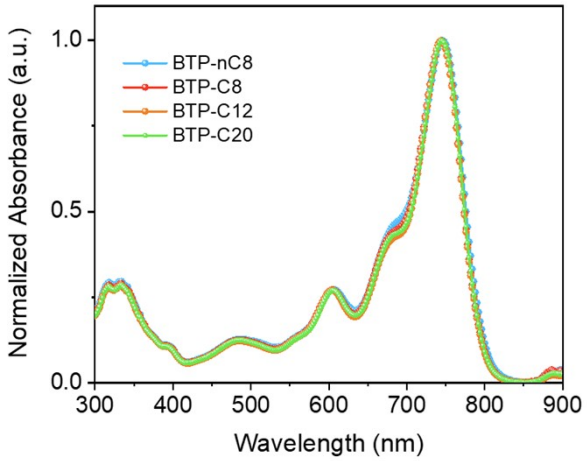

Fig. S19 UV-vis absorption spectra of BTP-nC8, BTP-C8, BTP-C12 and BTP-C20 in chloroform (10^{-5} M).

Table S1 Optical and electrochemical data of PM6, BTP-nC8, BTP-C8, BTP-C12 and BTP-C20.

	$\lambda_{sol.}$ [nm]	λ_{film} [nm]	λ_{onset} [nm]	E_g^{opt} [eV]	*E*onset ox/*E*onset red [V]	HOMO [eV]	LUMO [eV]
PM6	-	614	674	1.84	0.58/-1.79	-5.38	-3.01
BTP-nC8	745	794	883	1.40	0.93/-0.98	-5.73	-3.82
BTP-C8	745	819	889	1.39	0.94/-0.96	-5.74	-3.84
BTP-C12	745	828	889	1.39	0.95/-0.97	-5.75	-3.83
BTP-C20	745	809	873	1.42	0.96/-0.97	-5.76	-3.83

$E_g^{opt} = 1240/\lambda_{onset}$; HOMO = -(*E*onset ox + 4.80); LUMO = -(*E*onset red + 4.80). Noted that the electrochemical energy levels of PM6 and FREAs well agree with the reported values.[1,3]

7. GIWAXS of FREA neat films

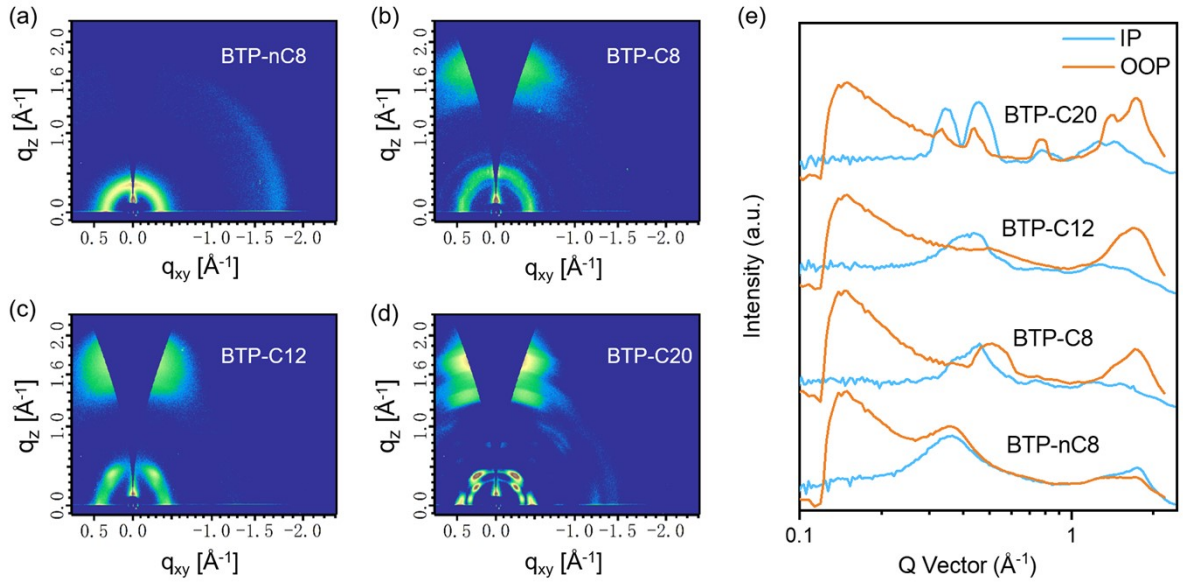

Fig. S20 2D GIWAXS patterns for (a) BTP-nC8, (b) BTP-C8, (c) BTP-C12 and (d) BTP-C20 neat films. (e) Corresponding GIWAXS intensity profiles along in-plane (IP) and out-of-plane (OOP) directions.

8. Contact angles

The surface tension can be evaluated by using the equation:[2]

$$\gamma_{LV}(1+cos\theta) = 4\frac{\gamma_S^d\gamma_L^d}{\gamma_S^d+\gamma_L^d} + 4\frac{\gamma_S^p\gamma_L^p}{\gamma_S^p+\gamma_L^p}$$

where γ_{LV} represents the surface tension of water/glycerol in equilibrium with its vapor. γ_L^d and γ_L^p represent the dispersion and polar components of the liquid surface tension, respectively, while γ_S^d and γ_S^p represent the dispersion and polar components of the solid surface tension, respectively. γ_S^d and γ_S^p can be calculated by using the contact angles with water and glycerol. The surface tension of donor and acceptors are calculated by the equation: $\gamma = \gamma_S^d + \gamma_S^p$. The closer the surface tension, the better miscibility between two materials.

Table S2 The parameters of contact angle measurement.

Name	θ_{water}[°]	$\theta_{glycerol}$[°]	γ [mN m^{-1}]	$\left(\sqrt{\gamma_{PM6}}-\sqrt{\gamma_{FREA}}\right)^2$
PM6	98.8	89.6	21.33	
BTP-nC8	97.8	82.2	26.59	0.290
BTP-C8	96.6	82.8	25.98	0.229
BTP-C12	97.4	83.3	25.37	0.175
BTP-C20	99.9	86.2	23.89	0.073

9. Device fabrication

The devices were fabricated with a structure of ITO/PEDOT:PSS/active layer/PDINN/Ag. The ITO glass substrates were cleaned by an ultrasonic cleaner in water with detergent, deionized water, acetone, and isopropyl alcohol for 15 min, successively, and subsequently treated with ultraviolet ozone generator for 20 min. Then, the PEDOT:PSS aqueous solution was spin-coated onto the ITO substrate with 4000 rpm for 30 s, and thermal annealed at 150 °C for 10 min. For active layer solution, the PM6:BTP-nC8, PM6:BTP-C8, PM6:BTP-C12, and PM6:BTP-C20 (w/w = 1:1.2, total 15 mg mL^{-1}) blends without/with additive were dissolved under 45 °C for 1h. The solution was spin-coated onto the top of PEDOT:PSS and followed by thermal annealing for 10 min to prepare the active layer. The electron transport layer, PDINN, (1.0 mg mL^{-1} in MeOH) was deposited onto the top of the active layer with 4000 rpm for 20 s. Finally, Ag (~100 nm) was evaporated onto the active layer under vacuum (pressure ca. 10^{-4} Pa) to afford the top electrode. Except for the fabrication of PEDOT:PSS layer, the other processes were all carried out in the nitrogen-filled glovebox.The effective area of the device is 0.04 cm^2.

Table S3 Photovoltaic parameters of OSCs based on PM6:BTP-nC8 with different D/A weight ratios under the illumination of AM1.5G (100 mA cm^{-2}).

D/A [w/w]	V_{OC} [V]	J_{SC} [mA cm^{-2}]	FF [%]	PCE [%]
1:1	0.861	23.76	67.9	13.91
1:1.2	0.855	24.27	69.0	14.33
1:1.4	0.848	24.51	66.0	13.73

Table S4 Photovoltaic parameters of OSCs based on PM6:BTP-nC8 (1:1.2, w/w) with different amounts of CN additive under the illumination of AM1.5G (100 mA cm^{-2}).

CN [v/v, %]	V_{OC} [V]	J_{SC} [mA cm^{-2}]	FF [%]	PCE [%]
0	0.855	24.27	69.0	14.33
0.25	0.857	26.01	71.4	15.93
0.5	0.828	25.64	71.7	14.66

Table S5 Photovoltaic parameters of OSCs based on PM6:BTP-nC8 (1:1.2, w/w, 0.25 vol% CN) at different thermal annealing temperatures under the illumination of AM1.5G (100 mA cm^{-2}).

Temperature [°C]	V_{OC} [V]	J_{SC} [mA cm^{-2}]	FF [%]	PCE [%]
80	0.857	26.01	71.4	15.93

100	0.846	26.23	70.30	15.66
120	0.843	26.44	70.40	15.69

Table S6 Photovoltaic parameters of OSCs based on PM6:BTP-C8 with different D/A weight ratios under the illumination of AM1.5G (100 mA cm^{-2}).

D/A [w/w]	V_{OC} [V]	J_{SC} [mA cm^{-2}]	FF [%]	PCE [%]
1:1	0.883	24.38	72.89	15.70
1:1.2	0.883	24.81	72.33	15.87
1:1.4	0.875	24.27	70.50	14.98

Table S7 Photovoltaic parameters of OSCs based on PM6:BTP-C8 (1:1.2, w/w) with different amounts of CN additive under the illumination of AM1.5G (100 mA cm^{-2}).

CN [v/v, %]	V_{OC} [V]	J_{SC} [mA cm^{-2}]	FF [%]	PCE [%]
0	0.883	24.81	72.33	15.87
0.25	0.882	26.37	72.13	16.78
0.5	0.871	25.67	72.74	16.27

Table S8 Photovoltaic parameters of OSCs based on PM6:BTP-C8 (1:1.2, w/w, 0.25 vol% CN) at different thermal annealing temperatures under the illumination of AM1.5G (100 mA cm^{-2}).

Temperature [℃]	V_{OC} [V]	J_{SC} [mA cm^{-2}]	FF [%]	PCE [%]
80	0.882	26.37	72.13	16.78
100	0.882	26.17	72.99	16.88
120	0.876	26.12	71.79	16.44

Table S9 Photovoltaic parameters of OSCs based on PM6:BTP-C12 with different D/A weight ratios under the illumination of AM1.5G (100 mA cm^{-2}).

D/A [w/w]	V_{OC} [V]	J_{SC} [mA cm^{-2}]	FF [%]	PCE [%]
1:1	0.885	22.14	73.50	14.41
1:1.2	0.891	23.17	75.11	15.51
1:1.4	0.887	23.86	72.21	15.29

Table S10 Photovoltaic parameters of OSCs based on PM6:BTP-C12 (1:1.2, w/w) with different amounts of CN additive under the illumination of AM1.5G (100 mA cm^{-2}).

CN [v/v, %]	V_{OC} [V]	J_{SC} [mA cm^{-2}]	FF [%]	PCE [%]
0	0.891	23.17	75.11	15.51
0.25	0.891	25.95	72.11	16.68
0.5	0.882	26.33	70.26	16.32

Table S11 Photovoltaic parameters of OSCs based on PM6:BTP-C12 (1:1.2, w/w, 0.25 vol% CN) at different thermal annealing temperatures under the illumination of AM1.5G (100 mA cm^{-2}).

Temperature [℃]	V_{OC} [V]	J_{SC} [mA cm^{-2}]	FF [%]	PCE [%]
80	0.891	25.95	72.11	16.68
100	0.888	26.03	73.10	16.91
120	0.882	26.26	72.38	16.77

Table S12 Photovoltaic parameters of OSCs based on PM6:BTP-C20 with different D/A weight ratios under the illumination of AM1.5G (100 mA cm^{-2}).

D/A [w/w]	V_{OC} [V]	J_{SC} [mA cm^{-2}]	FF [%]	PCE [%]
1:1	0.898	21.91	73.27	14.42
1:1.2	0.894	23.95	73.45	15.73
1:1.4	0.890	24.15	72.56	15.60

Table S13 Photovoltaic parameters of OSCs based on PM6:BTP-C20 (1:1.2, w/w) with different amounts of CN additive under the illumination of AM1.5G (100 mA cm^{-2}).

CN [v/v, %]	V_{OC} [V]	J_{SC} [mA cm^{-2}]	FF [%]	PCE [%]
0	0.894	23.95	73.45	15.73
0.25	0.907	25.73	70.30	16.42
0.5	0.880	26.09	70.70	16.24

Table S14 Photovoltaic parameters of OSCs based on PM6:BTP-C20 (1:1.2, w/w, 0.25 vol% CN) at different thermal annealing (TA) temperatures under the illumination of AM1.5G (100 mA cm^{-2}).

Temperature [°C]	V_{OC} [V]	J_{SC} [mA cm^{-2}]	FF [%]	PCE [%]
80	0.907	25.73	70.30	16.42
100	0.906	25.91	69.60	16.34
120	0.903	25.71	68.15	15.82

Electron-only devices

The structure of electron-only devices is ITO/ZnO/active layer/Ca/Al. The ZnO precursor was spin-coated onto ITO glass and annealed at 200 °C in air for 30 min. The active layer solution was deposited onto the ZnO layer in the glove box under N_2. Ca (~15 nm) and Al (~60 nm) were successively evaporated onto the active layer through a shadow mask (pressure ca. 10^{-4} Pa).

Hole-only devices

The structure of hole-only devices is ITO/PEDOT:PSS/active layer/MoO_3/Ag. A ~30 nm thick PEDOT:PSS layer was made via spin-coating an aqueous dispersion onto the ITO glass (4000 rpm for 30 s). The PEDOT:PSS substrate was dried at 150 °C for 10 min. The active layer solution was deposited onto the PEDOT:PSS layer in the glove box under N_2. Finally, MoO_3 (~3 nm) and Ag (~100 nm) were successively evaporated onto the active layer under a shadow mask (pressure ca. 10^{-4} Pa).

10. Bimolecular recombination

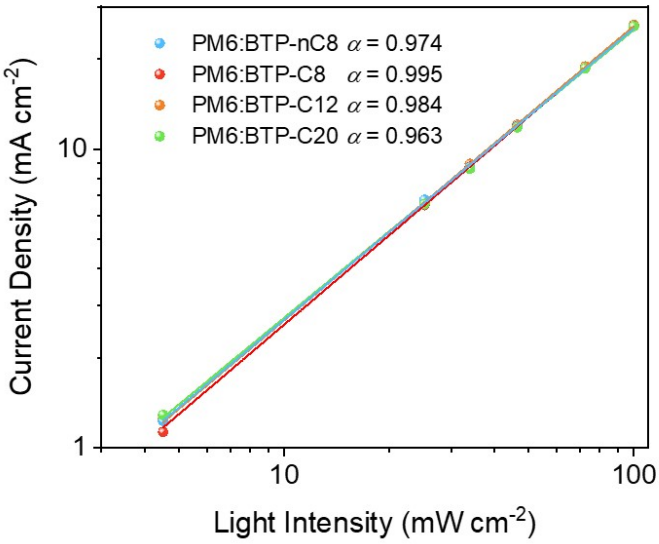

Fig. S21 Dependence of J_{SC} on light intensity for PM6:FREA based OSCs.

11. Space charge limited current (SCLC)

Charge carrier mobility was obtained by using the SCLC method. The mobility was determined by fitting the dark current to the model of a single carrier SCLC, which can be described as:

$$J = \frac{9}{8}\varepsilon_0\varepsilon_r\mu\frac{V^2}{d^3}$$

where J is the current density, μ is the zero-field mobility of electron (μ_e) or hole (μ_h), ε_0 is the permittivity of the vacuum, ε_r is the relative permittivity of the material, which is equal to 3.9 for electron-only devices and 3 for hole-only devices, d is the thickness of the blend film, and V is the effective voltage, $V = V_{appl} - V_{bi}$ (V_{appl} is the applied voltage, and V_{bi} is the built-in potential determined by electrode work function difference.).

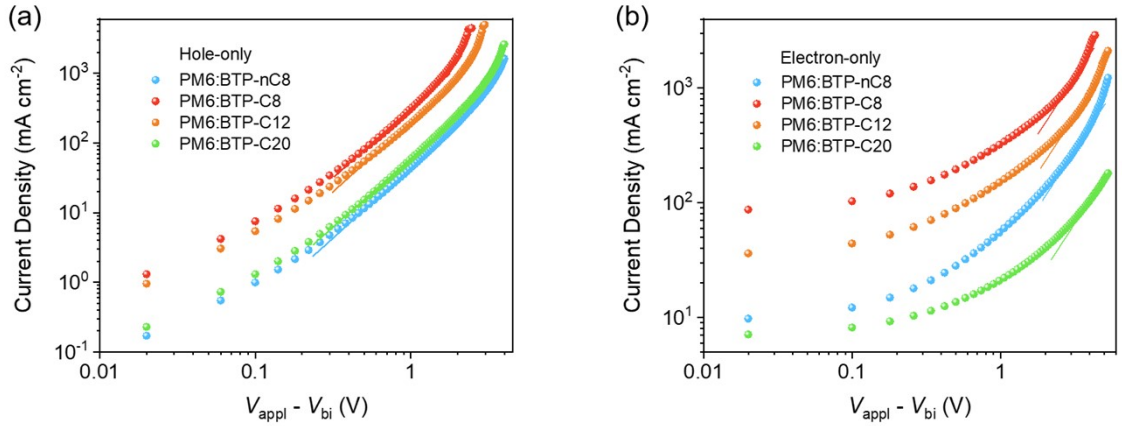

Fig. S22 Typical current density-applied voltage semi-log plots for hole-only devices (a) and electron-only devices (b) based on PM6:FREA blend films under dark. The measured data are shown as symbols, while the solid lines are the best fits to the SCLC model. Mobilities were extracted from the fitting.

Table S15 Charge carrier mobilities of devices based on PM6:FREA blend films.

PM6:FREA	μ_h (10^{-4} cm^2 V^{-1} s^{-1})	μ_e (10^{-4} cm^2 V^{-1} s^{-1})	μ_h/μ_e
PM6:BTP-nC8	1.13	1.57	0.72
PM6:BTP-C8	7.97	6.86	1.16
PM6:BTP-C12	4.91	3.06	1.60
PM6:BTP-C20	1.48	0.35	4.22

12. Resonant soft X-ray scattering (R-SoXS)

R-SoXS was measured at the beamline 11.0.1.2 of Advanced Light Source. All samples for R-SoXS measurements were prepared on the PEDOT:PSS modified ITO/glass substrate under the same conditions as those used for device fabrication and then transferred to the 100 nm thick, 1.5 mm×1.5 mm Si_3N_4 membrane (Norcada Inc., Canada) by floating in water. We collected the two-dimensional scattering patterns on an in-vacuum CCD camera (Princeton Instrument PI-MTE). The beam size for all samples is 200 mm by 100 mm.

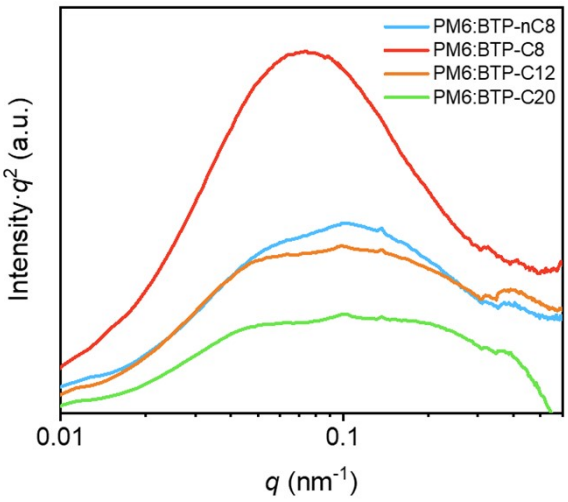

Fig. S23 R-SoXS profiles in log scale for PM6:FREA blend films.

13. Atomic force microscope

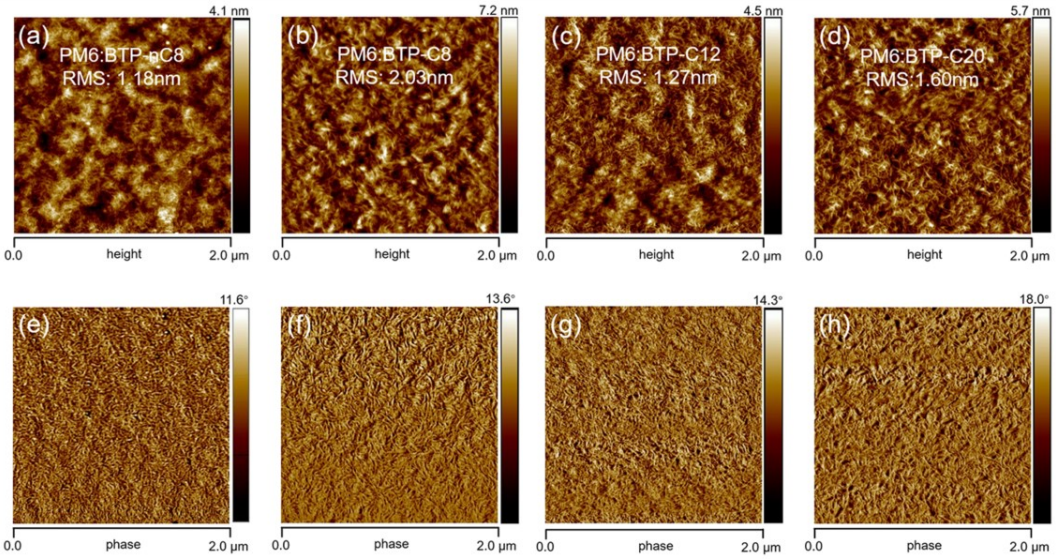

Fig. S24 (a-d) AFM height images of PM6:BTP-nC8, PM6:BTP-C8, PM6:BTP-C12 and PM6:BTP-C20 blend films. (e-h) AFM phase images of PM6:BTP-nC8, PM6:BTP-C8, PM6:BTP-C12 and PM6:BTP-C20 blend films.

14. Transient absorption (TA) spectroscopy

The laser source is a Ti:Sa amplified laser system (25 fs, 1 kHz, 800 nm, Legend Elite-1K-HE). The output pulse was split into two beams. The first beam was used to pump a tunable optical parametric amplifier (TOPAS-C, Light Conversion), which will output tunable femtosecond laser pulses from 350 nm to 2600 nm. The pulses centered at ~800 nm were selected as the excitation pulse to excite the FREA. The second beam with weaker energy was focused on an yttrium aluminum garnet plate to generate a white light continuum for the near-infrared probe. The time delay between the pump beam and the probe pulses was controlled by a motorized delay stage. TA spectrum was calculated from consecutive pump-on and pump-off measurements and averaged over 400 shots. All samples used TA measurements were prepared via spin-coating the solution onto the quartz substrate.

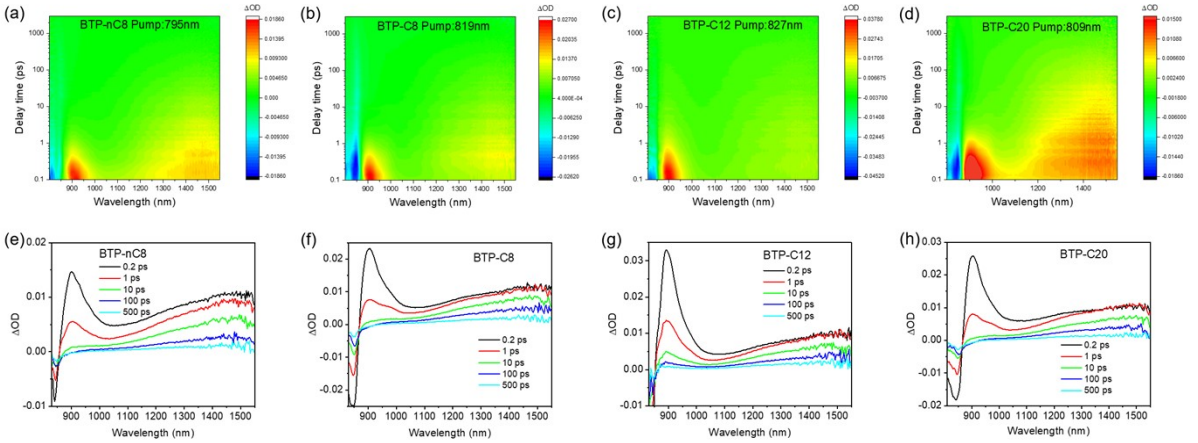

Fig. S25 (a)-(d) 2D color plots of femto-TA spectra of FREA neat films under excitation at the maximum absorption wavelength. (e)-(h) Representative femto-TA spectra of FREA neat films at indicated early delay times (< 500 ps).

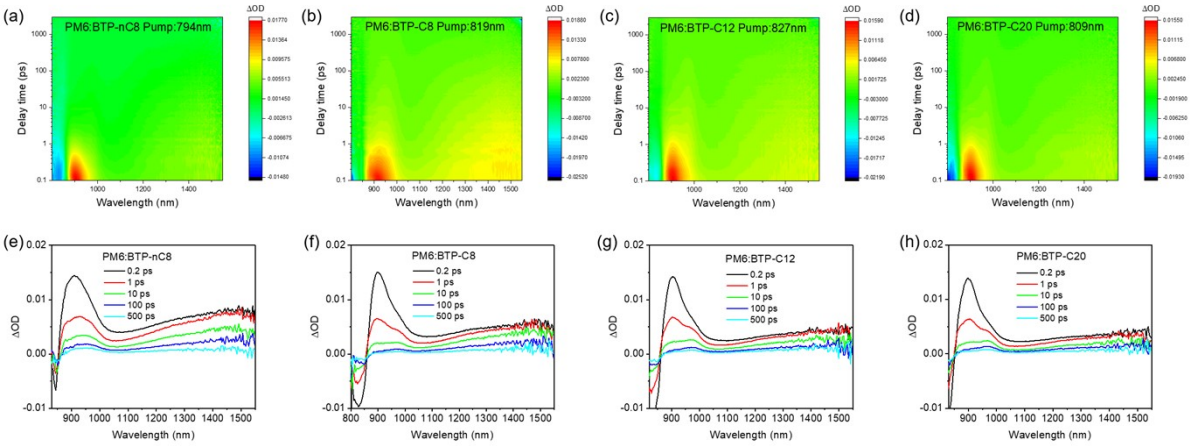

Fig. S26 (a)-(d) 2D color plots of femto-TA spectra of PM6:FREA blend films under excitation at the maximum absorption wavelength of the FREAs. (e)-(h) Representative femto-TA spectra of PM6:FREA blend films at indicated early delay times (< 500 ps).

References

[1] C. Li, J. Zhou, J. Song, J. Xu, H. Zhang, X. Zhang, J. Guo, L. Zhu, D. Wei, G. Han, J. Min, Y. Zhang, Z. Xie, Y. Yi, H. Yan, F. Gao, F. Liu and Y. Sun, *Nat. Energy* **2021**, 6, 605-613.

[2] J. Comyn, *Int. J. Adhes. Adhes.* **1990**, 12, 145-149.

[3] J. Liang, M. Pan, G. Chai, Z. Peng, J. Zhang, S. Luo, Q. Han, Y. Chen, A. Shang, F. Bai, Y. Xu, H. Yu, J. Y. L. Lai, Q. Chen, M. Zhang, H. Ade and H. Yan, *Adv. Mater.* **2020**, 32, 2003500.